Supporting Information

Contents

Section 1. Experimental section and methods

All starting materials, reagents and solvents used in experiments were commercially available, high-grade purity materials and used without further purification. Phosphomolybdic acid ($H_3PMo_{12}O_{40}·nH_2O$), cupric acetate monohydrate ($Cu(OAc)_2·H_2O$), hydrochloric acid (HCl, 36%), ammonium pervanadate (NH_4VO_3) and 1,2,4-triazolewere (Trz) purchased from Sinopharm Chemical Reagent Co., Ltd. Super-P carbon, polyvinylidene fluoride (PVDF) and 1-methyl-2-pyrrolidinone (NMP) and were purchased from Shenzhen Kejing Start Technology Co., Ltd. Elemental analyses for C, H, N were performed on a Perkin-Elmer 2400 CHN Elemental Analyzer. The IR spectrum was obtained on an Alpha Centaurt FT/IR spectrometer with KBr pellet in the 400-4000 cm^{-1} region. The XRPD patterns were obtained with a Rigaku D/max 2500V PC diffractometer with Cu-Kα radiation, the scanning rate is 5°/min, 2θ ranging from 5-50°. The thermogravimetric analyses (TGA) were carried out on a Perkin-Elmer-7 thermal analyzer at a heating rate of 10 °C·min^{-1}. SEM images were taken using Phenom ProX with an accelerating voltage of 15 kV. The simulated PXRD pattern was obtained based on the single-crystal data by diffraction crystal module of the Mercury (Hg) program version 3.3 available free of charge via the Internet at http://www.iucr.org/.

Synthesis of $[Co_7(Trz)_{12}(H_2O)_8][HPMo^{VI}_8Mo^V_4O_{40}(V^{IV}O)_2]·12H_2O$ (Co-PMo): Take 6ml H_2O and add 2ml PEG 400 forming surfactant aqueous solution assisted by ultrasound. Then $H_3PMo_{12}O_{40}$ (300 mg, 0.164 mmol), NH_4VO_3 (40mg, 0.342mmol) was dissolved in as-prepared surfactant aqueous solution at room temperature. Then $Co(NO_3)_2·6H_2O$ (200 mg, 0.687 mmol) and Trz ligand (80 mg, 1.16mmol) were added to the mixture and the pH value was then adjusted to about 4.3 using 1.0 mol·L^{-1} NaOH, which was transferred and sealed in a Teflon-lined autoclave (20mL) and kept at 170°C for 84 hours. After slow cooling to room temperature, we collected the black cuboid blocks. Yield: 34.5 % based on Co. Anal. calc for $C_{24}H_{64}Co_7Mo_{12}N_{36}O_{62}PV_2$: Calcd. C 8.13, H 1.82, N

14.22 %; Found C 8.11, H 1.78, N 14.10 %. IR (solid KBr pellet, ν/cm^{-1}, Fig. S11a): 3436 (VS), 1628 (S), 1512 (S), 1418 (W), 1286 (M), 1160 (W), 1057 (M), 948 (S), 870 (VS), 791 (W), 666 (W).

Synthesis of [Co$_7$(Trz)$_{12}$(H$_2$O)$_8$][HPW$^{VI}_8$W$^V_4$O$_{40}$(V^{IV}O)$_2$]·12H$_2$O (Co-PW): Take 2ml H$_2$O and add 2ml PEG 400 forming surfactant aqueous solution assisted by ultrasound. Then H$_3$PMo$_{12}$O$_{40}$ (300 mg, 0.164 mmol), NH$_4$VO$_3$ (40mg, 0.342mmol) was dissolved in as-prepared surfactant aqueous solution at room temperature. Then Co(NO$_3$)$_2$·6H$_2$O (200 mg, 0.687 mmol) and Trz ligand (80 mg, 1.16mmol) were added to the mixture and the pH value was then adjusted to about 4.3 using 1.0 mol·L^{-1} NaOH, which was transferred and sealed in a Teflon-lined autoclave (20mL) and kept at 170°C for 84 hours. After slow cooling to room temperature, we collected the black cuboid blocks. Yield: 34.5 % based on Co. Anal. calc for C$_{24}$H$_{64}$Co$_7$W$_{12}$N$_{36}$O$_{62}$PV$_2$: Calcd. C 6.27, H 1.40, N 10.96 %; Found C 6.24, H 1.34, N 10.89 %. IR (solid KBr pellet, ν/cm^{-1}, Fig. S11a): 3436 (VS), 1630 (S), 1508 (S), 1418 (W), 1291 (M), 1165 (M), 1075 (S), 956 (VS), 887 (W), 798 (VS), 668(W).

Preparation of nano-sized Co-PMo

Crystals of Co-PMo were ground for 5 h with an agate mortar and pestle. The resulted powder was dissolved in methanol and placed in a microwave digestion tank, which was heated in a microwave oven at 400 W for 4 h. The suspension of Co-PMo was separated by centrifugation, rinsed with water, and then dried in a vacuum drier at 80 °C for 24 h.

Fabrication of Co-PMo/SWCNTs

The Co-PMo/CNTs nanocomposites were synthesized using nano-sized Co-PMo crystals and SWCNTs by a simple sonication-driven functionalization strategy. SWCNTs loadings are chosen as 10, 20, 30 wt%, according to the total mass of the nanocomposites, referring as PCNT-1, PCNT -2, PCNT-3 respectively. In detail, purified single-walled CNTs (12mg, take 20 wt% for example) were dispersed in 20

mL of methanol under 60 kHz ultrasonication for 1 h at room temperature. Then, 48 mg of Nano-sized Co-PMo crystals in 1 mL acetonitrile was added to the CNTs dispersion and the dispersion was sonicated for another 2h. The resulting composite was isolated by centrifugation and dried at 60 ^{o}C overnight. The physically mixed Co-PMo and CNTs is prepared by grinding the mixture for 1h.

Cell Assembly and Electrochemical Measurements

Electrochemical lithium-storage properties of the synthesized materials were measured by using CR2025 coin-type test cells assembled in argon-filled glove box (the oxygen and water concentration maintained below 1 ppm). In order to avoid the influence of water molecules on battery performance, all samples were vacuum dried at 180 ^{o}C for 24 h. before being prepared into electrodes. To fabricate the working electrode, a slurry with appropriate viscosity consisting of 70wt% active materials, 20wt% Super-P carbon and 10wt % polyvinylidene fluoride (PVDF) binder dissolved in 1-methyl-2-pyrrolidinone was casted on the copper foil, drying at 80°C under vacuum for 24 h. The loading mass of electroactive materials on copper foil is about 1.2-1.4 mg/cm^2. The metallic lithium foil as the counter electrode, and 1.0 M LiPF6 in ethylene carbonate/diethyl carbonate (1:1 v/v) as the electrolyte. Galvanostatic charge/discharge cycles were performed on a LAND 2001A instrument (Wuhan, China) and electrochemical workstation (Princeton Applied Research, Germany) to record the circulation measurements, cyclic voltammetry (CV) and electrochemical impedance spectroscopy (EIS) of batteries at constant ambient temperature, respectively.

Section 2. Supplementary synthesized and structural information

μ_1 $\qquad$ $\mu_{1,2}$ $\qquad$ $\mu_{1,4}$ $\qquad$ $\mu_{1,2,4}$
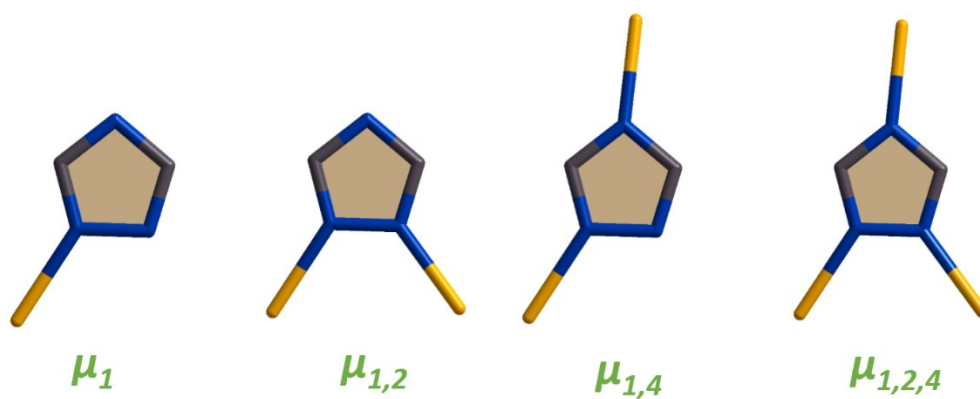
Scheme S1 The potential coordination modes of 1,2,4-triazole ligand (μ_1, $\mu_{1,2}$, $\mu_{1,4}$ and $\mu_{1,2,4}$).

Table S1 the synthesis strategies for crystalline hybrids.

Unit (mg)	PMo$_{12}$O$_{40}$	Co(NO$_3$)$_2$	1,2,4-trz	NH$_4$VO$_3$	surfactant*	Product
No.1	300	200	80	40	0	No crystal
No.2	300	200	80	40	SDBS	No crystal
No.3	300	200	80	40	PVP	No crystal
No.4	300	200	80	40	PEG 400	**Co-PMo**
No.5	300	200	80	40	PEG 600	No crystal
No.6	300	200	80	40	PEG 800	No crystal
No.7	300	200	80	40	PEG 1500	No crystal
No.8	300	200	80	40	PEG 2000	No crystal

* PEG = Polyethylene glycol 1500; SDBS = sodium dodecyl benzene sulfonate; PVP = polyvinylpyrrolidone. The dosage is 2 ml for both solid and liquid.

X-ray Crystallographic Study

Crystallographic data for as prepared crystals was collected on Bruker SMART-CCD diffractometer with monochromatic Mo-Kα radiation (λ = 0.71069 Å) at 296 K. The structures were solved by the direct method and refined full-matrix last squares on F2 through the SHELXTL and WINGX software package. The positions of hydrogen atoms on carbon atoms were calculated theoretically. The crystal data for Co-PMo and Co-PW are summarized in **Table S2**. The selected bond lengths and bond angles relative to the copper or vanadium sites are given in **Table S3**. Crystallographic data for the structure reported in this paper have been deposited in the Cambridge Crystallographic Data Center with CCDC Number 1877166 and 1935987.

Table S2 Crystal Data and Structure Refinements for **Co-PMo** and **Co-PW**

Compounds	Co-PMo	Co-PW
Formula	$C_{24}H_{64}Co_7Mo_{12}N_{36}O_{62}PV_2$	$C_{24}H_{64}Co_7W_{12}N_{36}O_{62}PV_2$
Fw	3545.645	4600.565
T (K)	293(2)	296(2) K
Crystal system	Tetragonal	Tetragonal
space group	$I\,4/m$	$I\,4/m$
a (Å)	17.795(5)	17.797 (4)
b (Å)	17.795(5)	17.797(4)
c (Å)	30.596(12)	30.1007(13)
α (º)	90	90
β (º)	90	90
γ (º)	90	90
V (Å³)	9689(7)	9533.9(6)
Z	4	4
D_c (g·cm⁻³)	2.431	3.205
μ (mm⁻¹)	2.969	15.910
$F(000)$	6840.0	8248.0
Theta range for data collection	1.324 to 26.039°	1.329 to 27.520°
Data / restraints / parameters	4886 / 12 / 342	5610 / 14 / 341
R_{int}	0.0516	0.0391
Final $R1^a$, $wR2^b$ [$I>\sigma(I)$]	0.0609, 0.1822	0.0607, 0.1783
Final $R1^a$, $wR2^b$(all data)	0.0680, 0.1902	0.0768, 0.1895

$^aR_1=\sum\left\|F_o\right|-\left|F_c\right\|/\sum\left|F_o\right|$ $^bwR_2 = \{\sum[w(F_o{}^2-F_c{}^2)^2]/\sum[w(F_o{}^2)^2]\}^{1/2}$
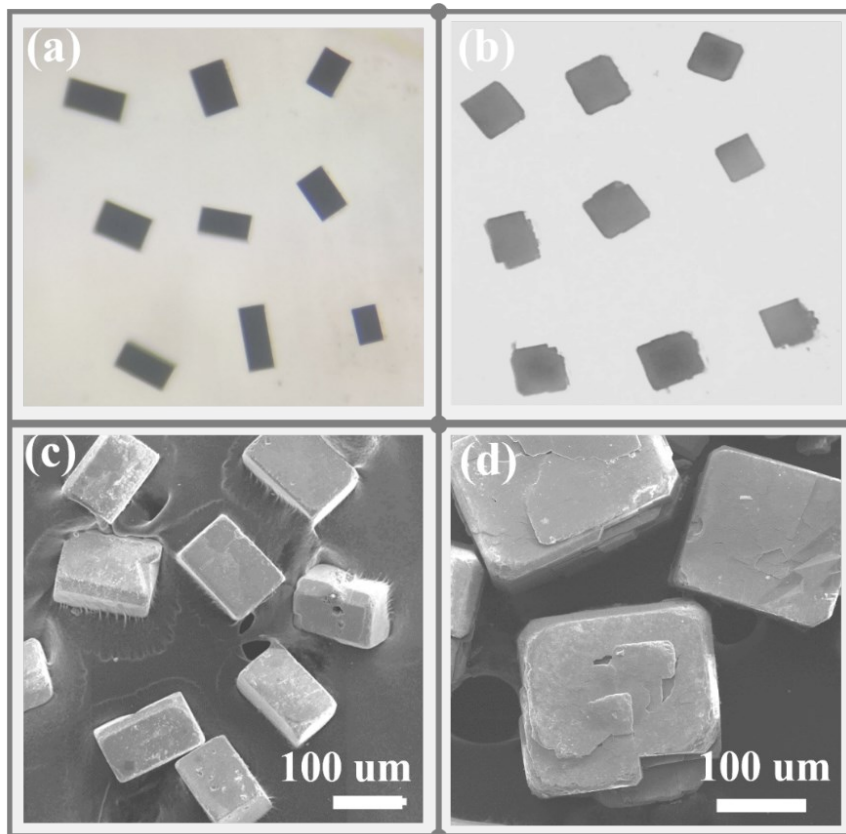
Fig. S1 The images of Co-PMo (left) and Co-PW (right) under (a, b) optical microscope and under (c, d) scanning electron microscope, respectively.
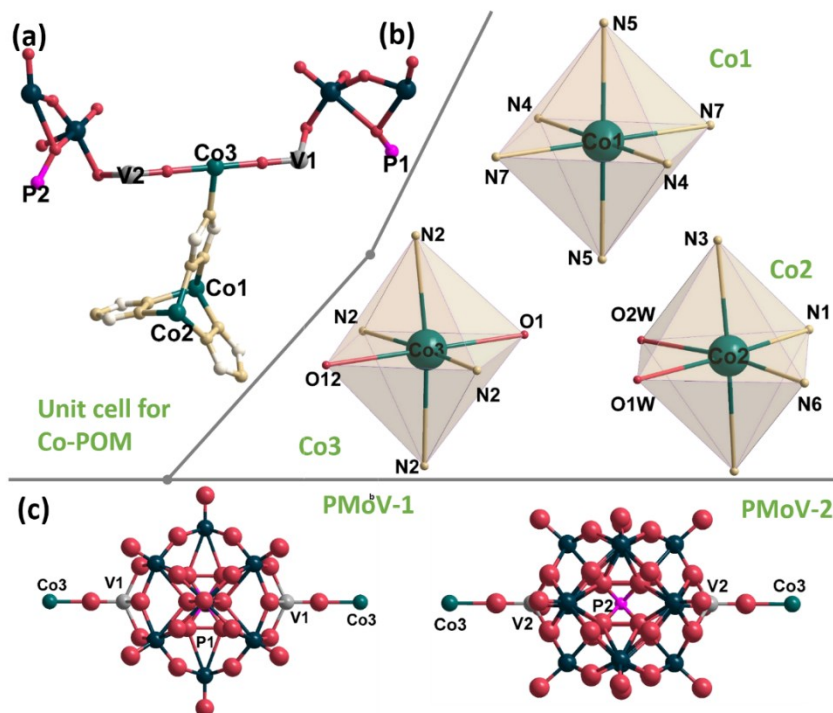
Fig. S2 (a) Ball/stick view of the crystallographic unit, (b) the coordination pattern of five crystallographic independent Co^{2+} cations, and (c) two $[PMo_{12}O_{40}(VO)_2]^{3-}$ polyanion. Co1 and Co4 cations connect to six nitrogen atoms originating from trz ligands, while Co2 and Co5 cations coordinate with four nitrogen atoms from trz ligands and two O atoms derived from water molecules, and Co3 cation link with four nitrogen atoms from trz ligands and two O atoms derived from two [VO] units.
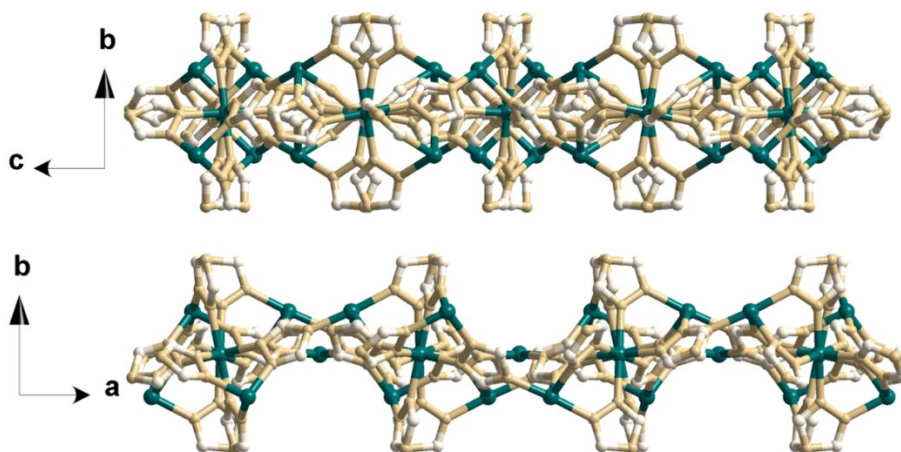
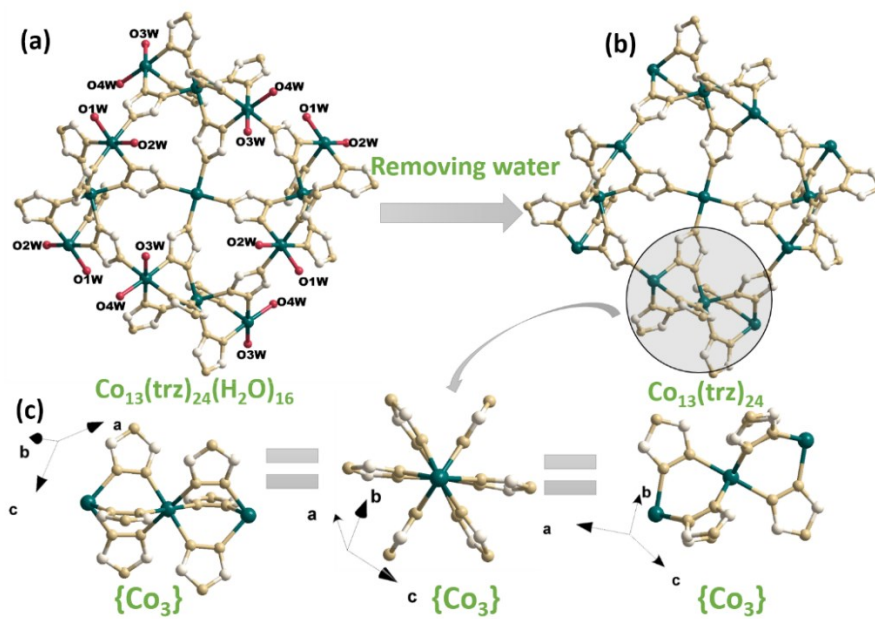**Fig. S3** View of two-dimensional layer $[Co_7(Trz)_{12}]n^{2n+}$ along [1 0 0] and [0 0 1] directions.

Fig. S4 (a, b) Ball/stick view of the positions of the water molecules in {Co$_{13}$} and (c) the connection modes in {Co$_3$} along different directions.
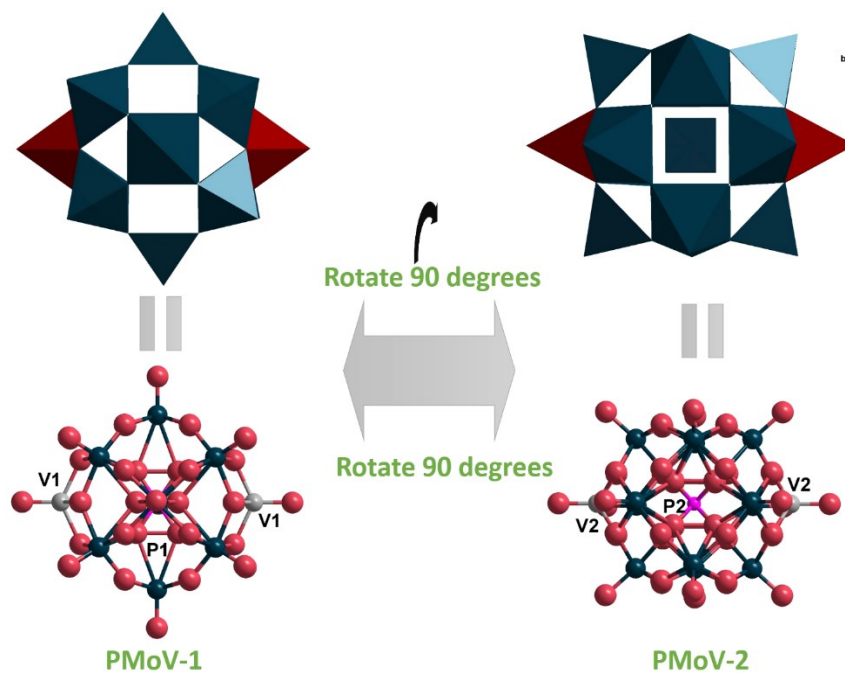
Fig. S5 View of two adjacent PMoV polyanions (PMoV-1 and PMoV-2) in 1 D PMoV-Co chains, which can transform each other by rotating 90 degrees.
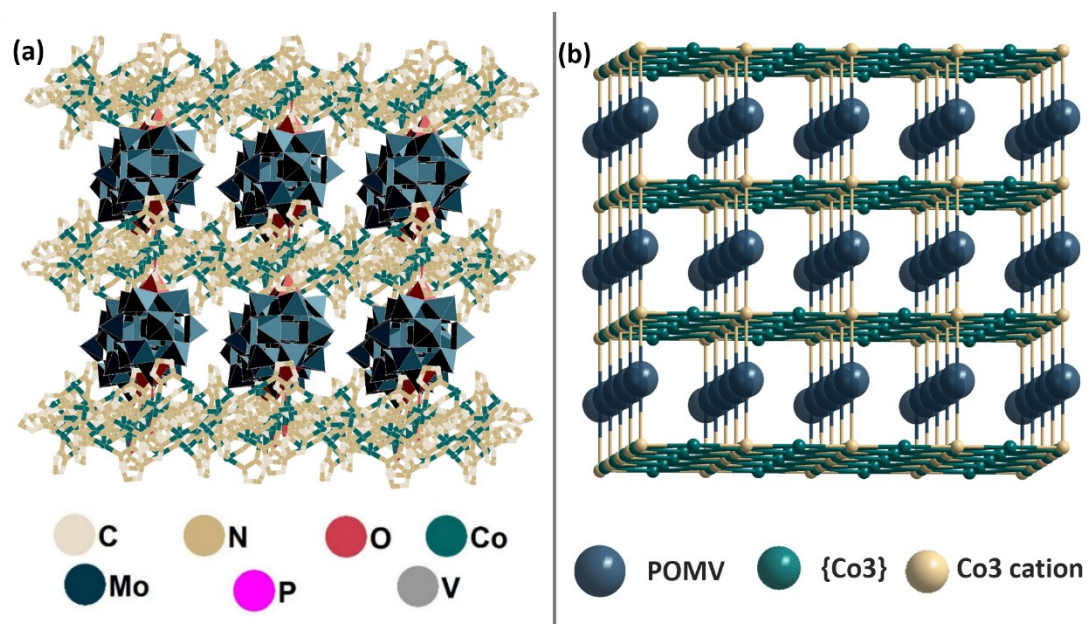
Fig. S6 (a) Combined ball/stick/polyhedral and (b) topologic representation of 3D POM-pillared frameworks of **Co-PMo** with opening hole.
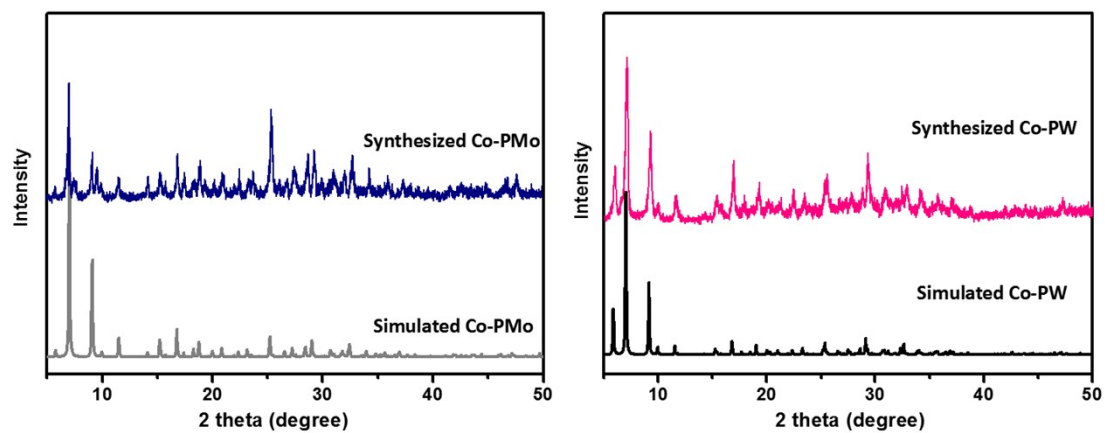
Section 3. Supplementary physical characterizations

Fig. S7 The PXRD patterns of **Co-PMo** and **Co-PW**: simulated pattern (below) and as-synthesized sample (up), respectively.
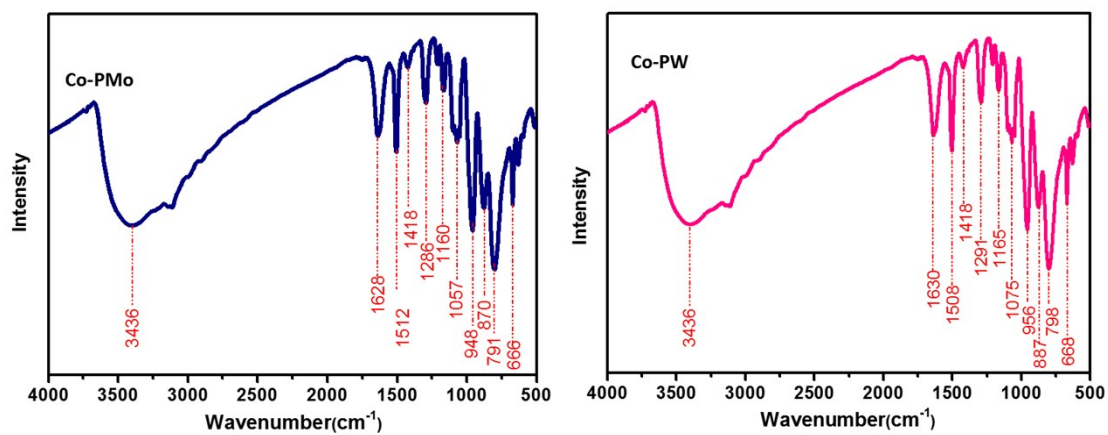
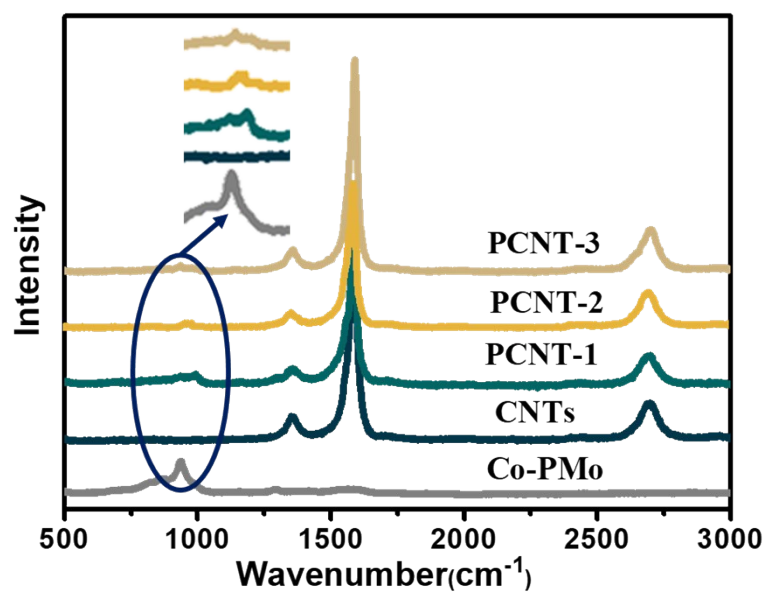**Fig. S8** FT-IR curves of **Co-PMo** and **Co-PW**, respectively.

Fig. S9 The Raman spectra of Co-PMo, CNTs and PCNT-n.
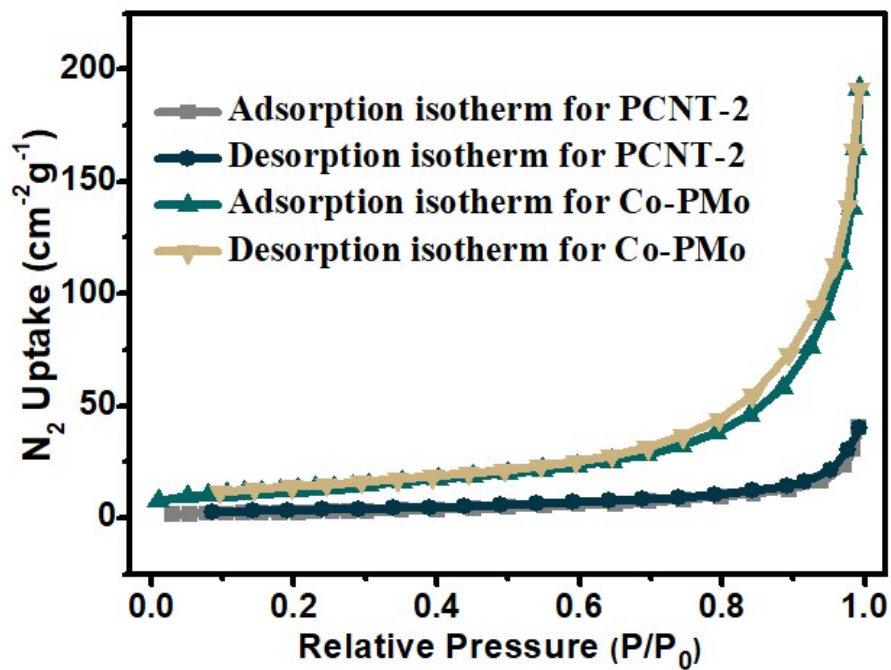
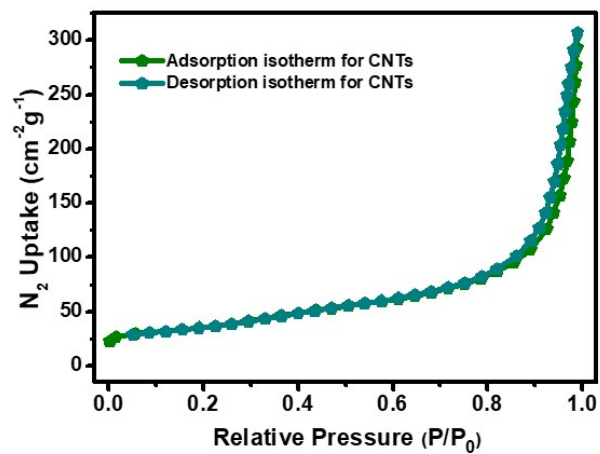**Fig. S10** N_2 adsorption-desorption isotherms of Co-PMo and PCNT-2.

Fig. S11 N_2 adsorption-desorption isotherms of CNTs.
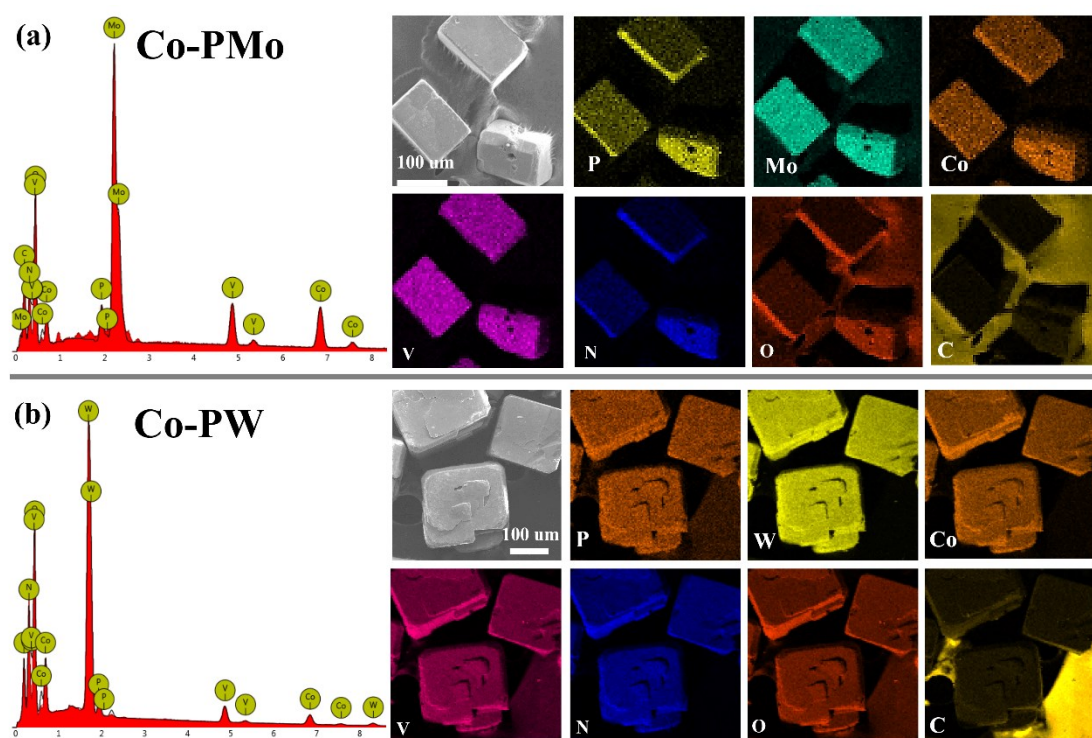
Fig. S12 The EDS spectrum, the SEM image and the elemental mapping images of (a) Co-PMo and (b) Co-PW.
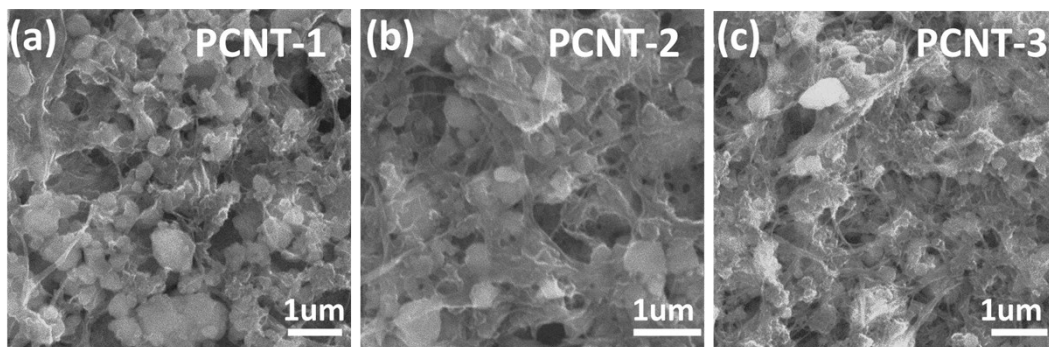
Fig. S13 SEM images of the as-synthesized (a) PCNT-1, (b) PCNT-2 and (c) PCNT-3.
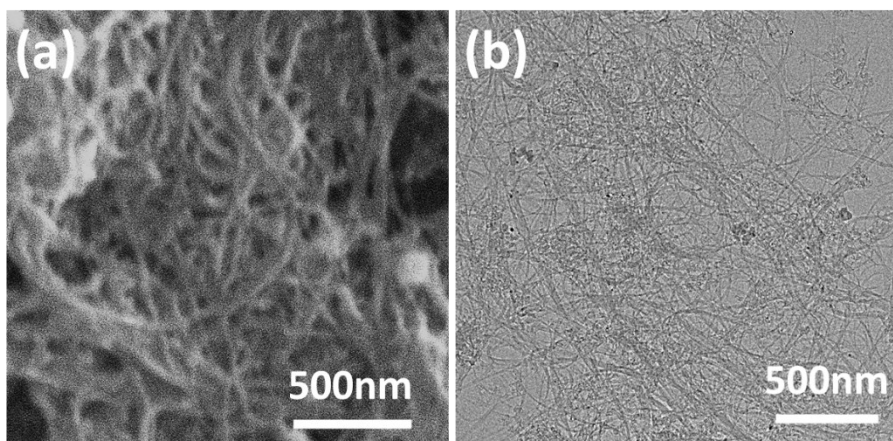
Fig. S14 (a) SEM image and (b) TEM image of CNTs.
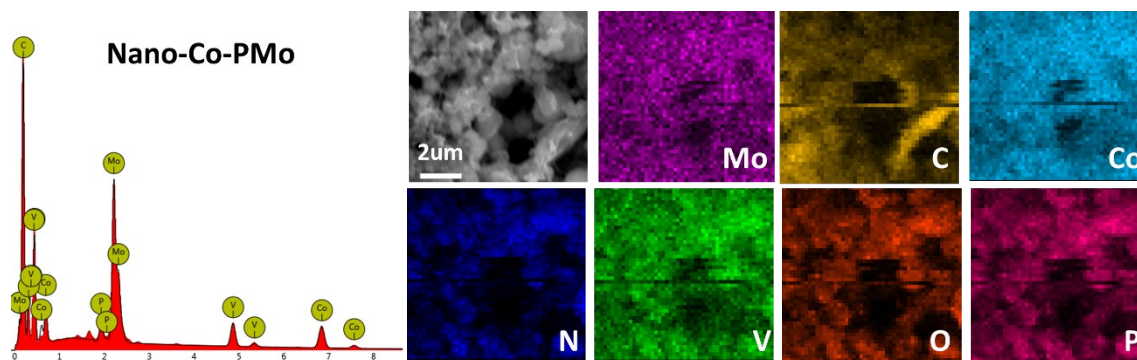
Fig. S15 The EDS spectrum, the SEM image and the elemental mapping images of PCNT-2.
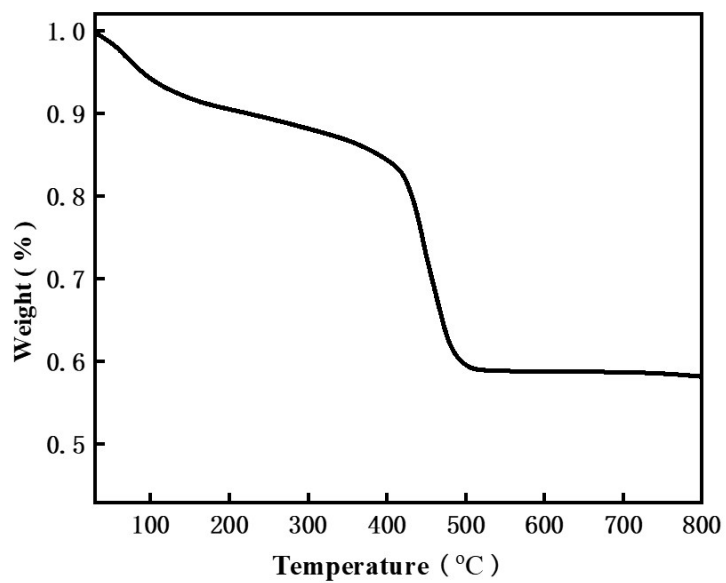
Fig. S16 The TGA curve of PCNT-2.

Section 4. Additional electrochemical experiments
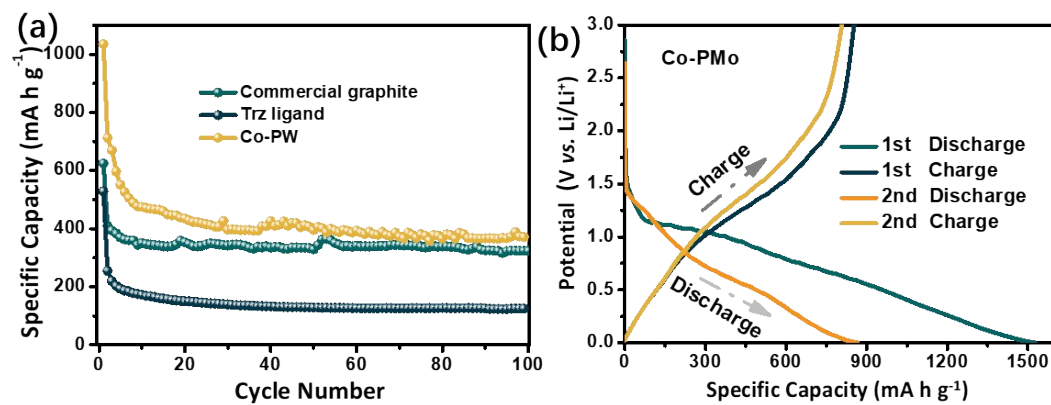
Fig. S17 Electrochemical performance differen electrodes. (a) Cycling performance at a current density of 100 mA g^{-1}. (b) Charge/discharge profiles for different cycles for Co-PMo.
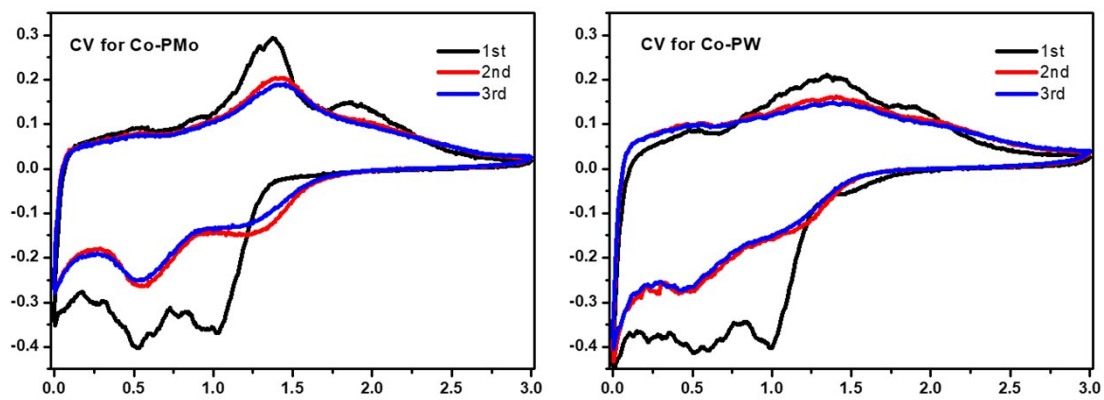
Fig. S18 Cyclic voltammetry of the Co-PMo and Co-PW anodes at the range of 0.01-3 V (scan rate: 0.1 mV s^{-1}).
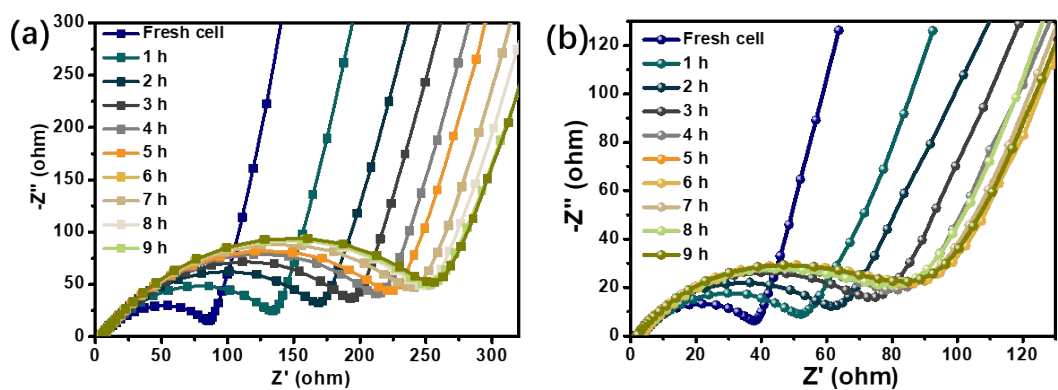
Fig. S19 Nyquist plots of fresh cell prolonged storage for (a) Co-PMo and (b) PCNT-2 electrode.

The theoretical capacities of POMOF was calculated according to **equation S1**:

$$Q = nF/3.6M = 96500n/3.6M \qquad \textbf{equation S1}$$

Where Q is the reversible charging–discharging capacity, n is the number of electrons passed during the redox reaction, and M is the molecular weight.

(1) Calculation of the theoretical capacities of POMs:

When Li^+ intercalate/deintercalate into the structure of PMo_{12}, we based on the redox reactions of Mo atoms which are due to the intercalation mechanism for Li storage (equations S2) and the XPS results.


$$Mo^{6+} \leftrightarrow Mo^{4+} \qquad \textbf{equation S2}$$
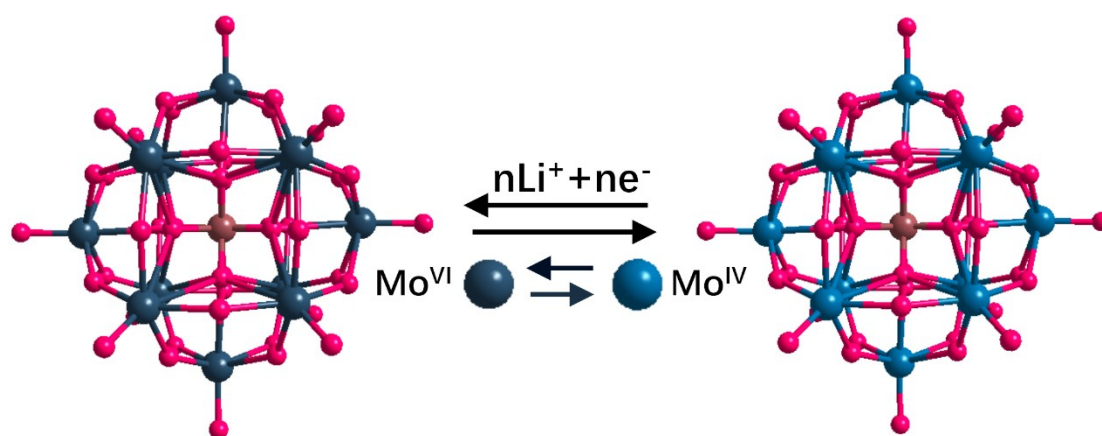
If twelve Mo^{6+} are all reduced to Mo^{4+}, maximum of $n = 24$, $Q_{POM} = 328.88$ mA h g^{-1}.

(2) Calculation of the theoretical capacities of MOFs:

If redox reactions where Cu^{2+} transformed into Cu^+ occurred in Cu-based POMOFs because of the intercalation mechanism for Li storage. On the other hand, possible lithiation/delithiation sites for coordination with Li such as the N atoms in Trz ligands of POMOF.

S26
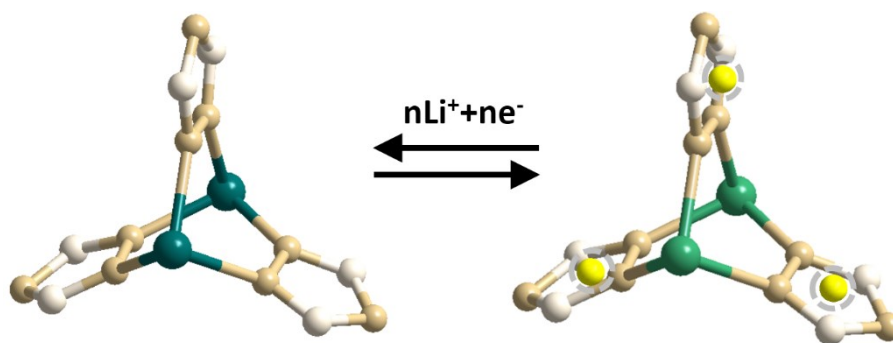
As seen in Schematic S1, one Li$^+$ maybe coordinate with one Trz ligand, thus, in MOF, n = 12, Q_{MOF} = 238.17 mA h g^{-1}. However, further investigations are necessary to understand the exact mechanism in this case.

(3) Calculation of the theoretical capacities of Co-PMo:

After removing water molecules, the molecular formula of **Co-PMo** is [Co$_7$(Trz)$_{12}$][HPMo$_{12}$O$_{42}$V$_2$]. And based on the discussions above, here the maximum of n = 12 + 20 = 34, $Q_{\textbf{Co-PMo}}$ = 325.13 mA h g^{-1}.

(4) Calculation of the theoretical capacities of PCNT-2:

The PCNT-2 nanocomposite contains 80% Co-POM and 20% single-walled carbon nanotubes. According to the measured capacity of carbon nanotubes is 418 mA h g^{-1}, here $Q_{\textbf{PCNT-2}}$ = 325.13 mA h g^{-1}·0.8+415 mA h g^{-1}·0.2 = 343.10 mA h g^{-1}.
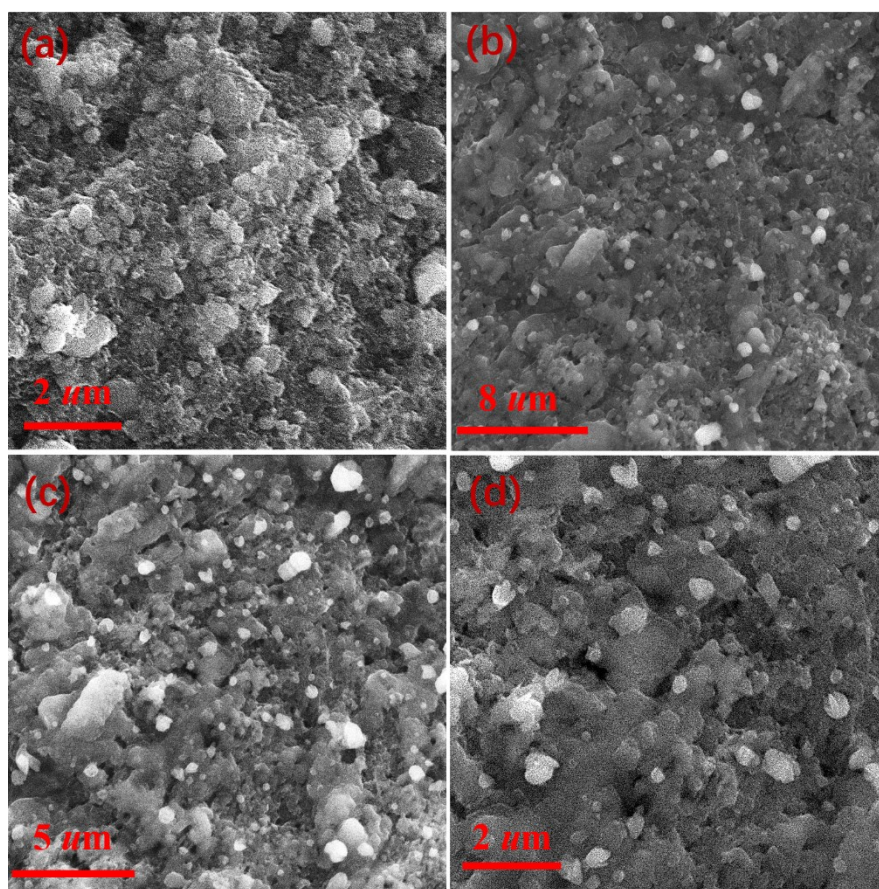
Fig. S20 SEM image of PCNT-2 before (a) and after discharge/charge (b, c and d) reactions (all of them mixed with 20%wt Super-P carbon and 10%wt PVDF).
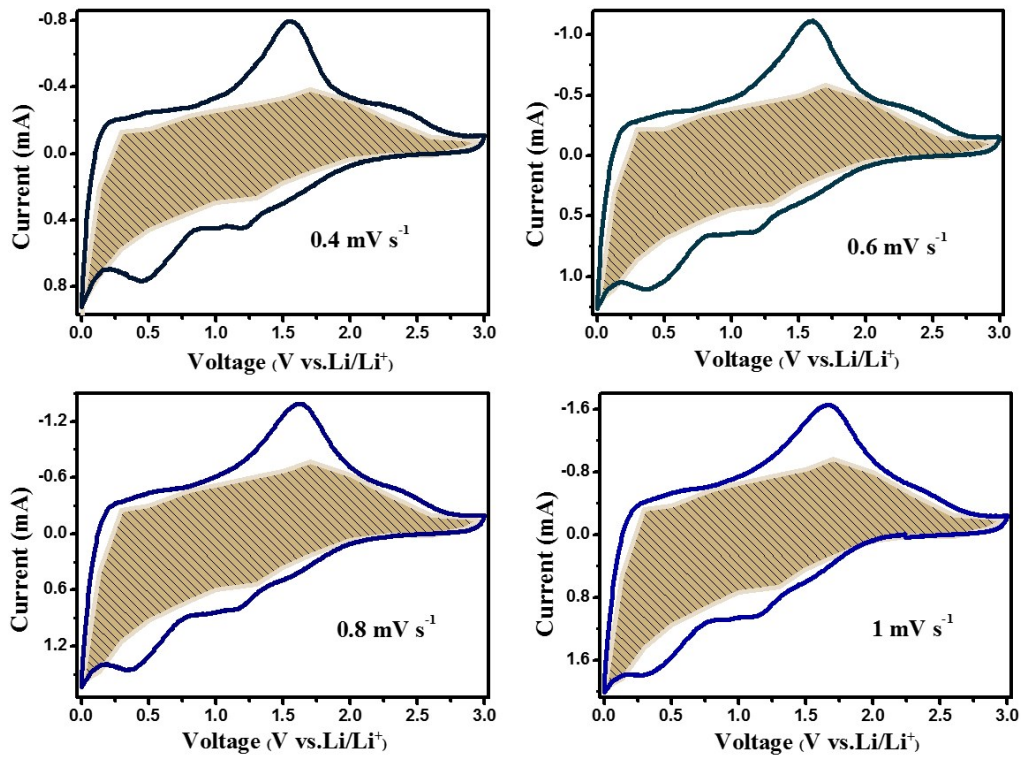
Fig. S21 Capacitive controlled charge storage contributions separated with cyclic voltammograms at 0.4, 0.6, 0.8 and 1 mV s^{-1} scan of the fresh PCNT-2 cell.

Fig. S22 Capacitive controlled charge storage contributions separated with cyclic voltammograms at 0.4, 0.6, 0.6 and 1 mV s^{-1} scan of PCNT-2 cell after 50 cycles.

Section 5. Selected bonds lengths and angles for compounds

Table S3 Selected bonds lengths (Å) and angles (°) for Co-PMo.

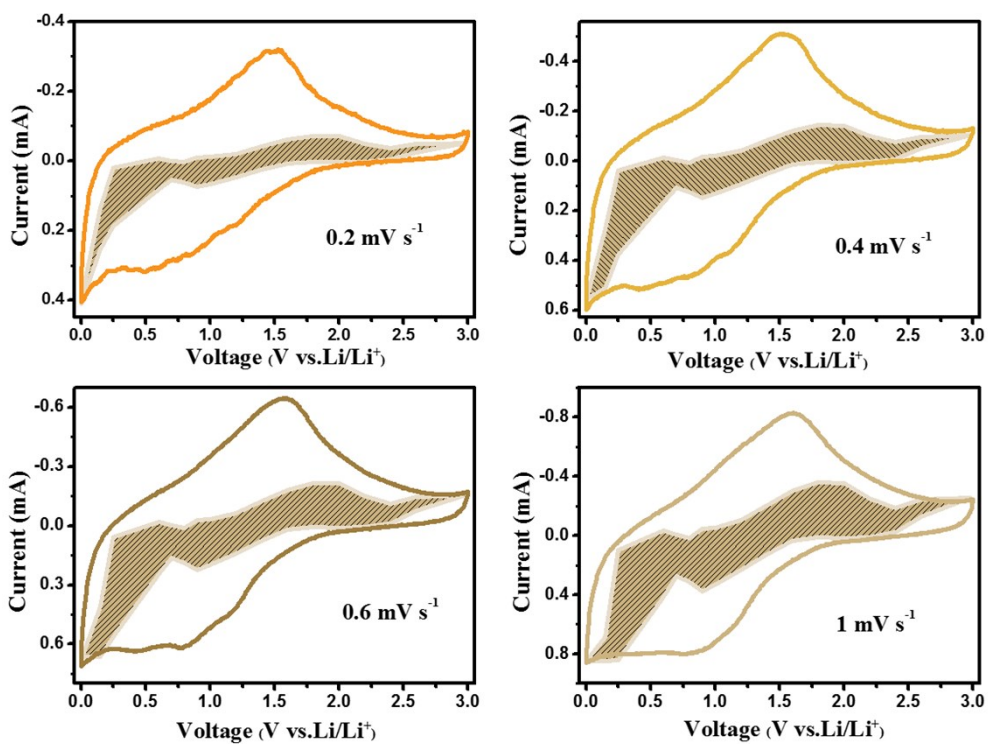|			
N(1)-Co(2)	2.091(9)	N(17)-Co(4)	2.203(10)
N(2)-Co(3)	2.128(9)	N(18)-Co(5)	2.161(9)
N(3)-Co(3)	2.125(8)	O(1)-V(1)	1.606(11)
N(4)-N(10)	1.378(13)	O(1)-Co(3)	2.028(11)
N(4)-Co(5)	2.088(9)	O(13)-V(2)	1.936(9)
N(5)-Co(2)	2.135(9)	O(14)-V(2)	1.935(9)
N(6)-Co(5)	2.130(8)	O(14)-Mo(1)	2.047(9)
N(7)-Co(1)	2.140(8)	O(18)-V(2)	1.610(11)
N(8)-Co(4)	2.142(8)	O(18)-Co(3)	2.081(11)
N(9)-Co(1)	2.118(9)	O(22)-V(1)	1.918(9)
N(10)-Co(4)	2.112(8)	O(23)-V(1)	1.926(9)
N(11)-Co(5)	2.097(9)	V(1)-O(22)#5	1.918(9)
N(12)-Co(1)	2.191(10)	V(1)-O(23)#5	1.926(9)
N(13)-Co(2)	2.161(9)	V(2)-O(14)#5	1.935(9)
N(14)-Co(2)	2.093(9)	V(2)-O(13)#5	1.936(9)
N(9)-Co(1)-N(9)#9	180	N(11)-Co(5)-N(6)	96.7(4)
N(9)-Co(1)-N(7)#9	90.6(3)	N(4)-Co(5)-O(3W)	90.2(4)
N(9)#9-Co(1)-N(7)#9	89.4(3)	N(11)-Co(5)-O(3W)	172.1(4)
N(9)-Co(1)-N(7)	89.4(3)	N(6)-Co(5)-O(3W)	87.9(4)
N(9)#9-Co(1)-N(7)	90.6(3)	N(4)-Co(5)-O(4W)	174.1(4)
N(7)#9-Co(1)-N(7)	180	N(11)-Co(5)-O(4W)	89.8(4)
N(9)-Co(1)-N(12)	91.0(4)	N(6)-Co(5)-O(4W)	88.8(4)
N(9)#9-Co(1)-N(12)	89.0(3)	O(3W)-Co(5)-O(4W)	83.9(4)
N(7)#9-Co(1)-N(12)	89.7(3)	N(4)-Co(5)-N(18)	89.2(4)
N(7)-Co(1)-N(12)	90.3(3)	N(11)-Co(5)-N(18)	87.6(4)
N(9)-Co(1)-N(12)#9	89.0(3)	N(6)-Co(5)-N(18)	175.7(4)
N(9)#9-Co(1)-N(12)#9	91.0(4)	O(3W)-Co(5)-N(18)	87.9(4)
N(7)#9-Co(1)-N(12)#9	90.3(3)	O(4W)-Co(5)-N(18)	91.1(4)
N(7)-Co(1)-N(12)#9	89.7(3)	O(1)-V(1)-O(22)#5	115.1(3)
N(12)-Co(1)-N(12)#9	180	O(1)-V(1)-O(22)	115.1(3)
N(1)-Co(2)-N(14)	96.5(4)	O(22)#5-V(1)-O(22)	129.7(7)
N(1)-Co(2)-N(5)	90.5(3)	O(1)-V(1)-O(23)#5	115.0(3)
N(14)-Co(2)-N(5)	96.6(4)	O(22)#5-V(1)-O(23)#5	79.7(4)
N(1)-Co(2)-O(2W)	90.2(4)	O(22)-V(1)-O(23)#5	79.7(4)
N(14)-Co(2)-O(2W)	171.8(4)	O(1)-V(1)-O(23)	115.0(3)
N(5)-Co(2)-O(2W)	88.1(4)	O(22)-V(1)-O(23)	79.7(4)
N(1)-Co(2)-O(1W)	174.2(4)	O(23)#5-V(1)-O(23)	130.1(7)
N(14)-Co(2)-O(1W)	89.4(4)	O(18)-V(2)-O(14)	113.5(3)

N(5)-Co(2)-O(1W)	88.7(4)	O(18)-V(2)-O(14)#5	113.5(3)
O(2W)-Co(2)-O(1W)	84.0(4)	O(14)-V(2)-O(14)#5	133.1(6)
N(1)-Co(2)-N(13)	88.7(4)	O(18)-V(2)-O(13)	113.1(3)
N(14)-Co(2)-N(13)	87.6(4)	O(14)-V(2)-O(13)	80.9(4)
N(5)-Co(2)-N(13)	175.7(4)	O(14)#5-V(2)-O(13)	81.1(4)
O(2W)-Co(2)-N(13)	87.8(4)	O(18)-V(2)-O(13)#5	113.1(3)
O(1W)-Co(2)-N(13)	91.8(4)	O(14)-V(2)-O(13)#5	81.1(4)
O(1)-Co(3)-O(18)	180	O(14)#5-V(2)-O(13)#5	80.9(4)
O(1)-Co(3)-N(3)#5	93.7(2)	O(13)-V(2)-O(13)#5	133.7(7)
O(18)-Co(3)-N(3)#5	86.3(3)	N(10)#2-Co(4)-N(17)#2	90.7(3)
O(1)-Co(3)-N(3)	93.7(3)	N(8)#2-Co(4)-N(17)#2	89.3(3)
O(18)-Co(3)-N(3)	86.3(2)	N(8)-Co(4)-N(17)#2	90.7(3)
N(3)#5-Co(3)-N(3)	172.6(5)	N(10)-Co(4)-N(17)	90.7(3)
O(1)-Co(3)-N(2)	93.6(3)	N(10)#2-Co(4)-N(17)	89.3(3)
O(18)-Co(3)-N(2)	86.4(3)	N(8)#2-Co(4)-N(17)	90.7(3)
N(3)#5-Co(3)-N(2)	89.9(3)	N(8)-Co(4)-N(17)	89.3(3)
N(3)-Co(3)-N(2)	89.6(3)	N(17)#2-Co(4)-N(17)	180
O(1)-Co(3)-N(2)#5	93.6(3)	N(4)-Co(5)-N(11)	96.1(4)
O(18)-Co(3)-N(2)#5	86.4(3)	N(4)-Co(5)-N(6)	90.4(4)
N(3)#5-Co(3)-N(2)#5	89.6(3)	N(10)#2-Co(4)-N(8)#2	90.6(3)
N(3)-Co(3)-N(2)#5	89.9(3)	N(10)-Co(4)-N(8)	90.6(3)
N(2)-Co(3)-N(2)#5	172.7(5)	N(10)#2-Co(4)-N(8)	89.4(3)
N(10)-Co(4)-N(10)#2	180.0(5)	N(8)#2-Co(4)-N(8)	180
N(10)-Co(4)-N(8)#2	89.4(3)	N(10)-Co(4)-N(17)#2	89.3(3)

Symmetry transformations used to generate equivalent atoms: #1 x-1/2,-y+1/2,z; #2 -x+3/2,-y+1/2,-z+2;   #3 x+1/2,-y+1/2,z; #4 -x+1,-y+1,-z+1; #5 -x+1,y,-z+1; #6 x,-y+1,z; #7 x,-y,z; #8 -x+1,-y,-z+1; #9 -x+3/2,-y+1/2,-z+1.

Table S4 Selected bonds lengths (Å) and angles (°) for Co-PW.

V(2)-O(12)#1	1.975(13)	N(1)-Co(1)	2.099(10)
V(2)-O(12)#2	1.975(13)	N(2)-Co(2)	2.102(10)
V(2)-O(12)#3	1.975(13)	N(3)-Co(3)	2.132(10)
V(2)-O(12)	1.975(13)	N(4)-C(5)#5	1.324(15)
V(1)-O(2)	1.52(3)	N(4)-N(5)	1.368(15)
V(1)-O(6)#3	1.980(14)	N(4)-Co(1)	2.095(11)
V(1)-O(6)#2	1.980(14)	N(5)-Co(2)	2.134(10)
V(1)-O(6)#1	1.980(14)	N(6)-Co(1)	2.156(11)
V(1)-O(6)	1.980(14)	N(7)-Co(2)	2.147(12)
Co(1)-O(2W)	2.146(11)	O(1)-Co(3)	2.09(2)
Co(1)-O(1W)	2.165(11)	O(2)-Co(3)	2.03(2)
Co(3)-N(3)#3	2.132(10)	Co(1)-N(9)	2.136(10)
Co(3)-N(3)#1	2.132(10)	Co(3)-N(3)#2	2.132(10)
O(1)-V(2)-O(12)#1	111.7(6)	N(1)-Co(1)-O(1W)	175.0(4)
O(1)-V(2)-O(12)#2	111.7(6)	N(9)-Co(1)-O(1W)	88.6(5)
O(12)#1-V(2)-O(12)#2	82.2(4)	O(2W)-Co(1)-O(1W)	83.3(5)
O(1)-V(2)-O(12)#3	111.7(6)	N(6)-Co(1)-O(1W)	92.4(5)
O(12)#1-V(2)-O(12)#3	82.2(4)	O(2)-Co(3)-O(1)	180
O(12)#2-V(2)-O(12)#3	136.7(12)	O(2)-Co(3)-N(3)	93.2(3)
O(12)#1-V(2)-O(12)	136.7(12)	O(1)-Co(3)-N(3)	86.8(3)
O(12)#2-V(2)-O(12)	82.2(4)	O(2)-Co(3)-N(3)#3	93.2(3)
O(12)#3-V(2)-O(12)	82.2(4)	O(1)-Co(3)-N(3)#3	86.8(3)
O(2)-V(1)-O(6)#3	114.2(7)	N(3)-Co(3)-N(3)#3	89.82(3)
O(2)-V(1)-O(6)#2	114.2(7)	O(2)-Co(3)-N(3)#2	93.2(3)
O(6)#3-V(1)-O(6)#2	131.5(13)	O(1)-Co(3)-N(3)#2	86.8(3)
O(2)-V(1)-O(6)#1	114.2(7)	N(3)-Co(3)-N(3)#2	89.82(3)
O(6)#3-V(1)-O(6)#1	80.3(5)	N(3)#3-Co(3)-N(3)#2	173.6(6)
O(6)#2-V(1)-O(6)#1	80.3(5)	O(2)-Co(3)-N(3)#1	93.2(3)
O(2)-V(1)-O(6)	114.2(7)	O(1)-Co(3)-N(3)#1	86.8(3)
O(6)#3-V(1)-O(6)	80.3(5)	N(3)-Co(3)-N(3)#1	173.6(6)
O(6)#2-V(1)-O(6)	80.3(5)	N(3)#3-Co(3)-N(3)#1	89.82(3)
O(6)#1-V(1)-O(6)	131.5(13)	N(3)#2-Co(3)-N(3)#1	89.82(3)
N(4)-Co(1)-N(1)	95.8(4)	N(2)-Co(2)-N(2)#14	180
N(4)-Co(1)-N(9)	96.3(4)	N(2)-Co(2)-N(5)	89.2(4)
N(1)-Co(1)-N(9)	90.5(4)	N(2)#14-Co(2)-N(5)	90.8(4)
N(4)-Co(1)-O(2W)	170.4(5)	N(2)-Co(2)-N(5)#14	90.8(4)
N(1)-Co(1)-O(2W)	91.8(5)	N(2)#14-Co(2)-N(5)#14	89.2(4)
N(9)-Co(1)-O(2W)	89.5(4)	N(5)-Co(2)-N(5)#14	180
N(4)-Co(1)-N(6)	87.2(4)	N(2)-Co(2)-N(7)	90.5(4)
N(1)-Co(1)-N(6)	88.2(4)	N(2)#14-Co(2)-N(7)	89.5(4)
N(9)-Co(1)-N(6)	176.3(4)	N(5)-Co(2)-N(7)	89.7(4)

O(2W)-Co(1)-N(6)	87.1(5)	N(5)#14-Co(2)-N(7)	90.3(4)
N(4)-Co(1)-O(1W)	89.2(5)	N(2)-Co(2)-N(7)#14	89.5(4)
N(5)#14-Co(2)-N(7)#14	89.7(4)	N(2)#14-Co(2)-N(7)#14	90.5(4)
N(7)-Co(2)-N(7)#14	180.00(13)	N(5)-Co(2)-N(7)#14	90.3(4)

Symmetry transformations used to generate equivalent atoms: #1 -x+1,-y+1,z; #2 y,-x+1,z; #3 -y+1,x,z; #4 -y+1/2,x-1/2,-z+1/2; #5 y+1/2,-x+1/2,-z+1/2; #6 y,-x+1,-z+1; #7 -y+1,x,-z+1; #8 x,y,-z+1; #9 -x+1,-y+1,-z+1; #10 -y+1,x,-z; #11 x,y,-z; #12 y,-x+1,-z; #13 -x+1,-y+1,-z; #14 -x+3/2,-y+1/2,-z+1/2.